



Published in final edited form as:

Science. 2008 October 17; 322(5900): 460–464. doi:10.1126/science.1163673.

Innate immunity in *Caenorhabditis elegans* is regulated by neurons expressing NPR-1/GPCR

Katie L. Styer¹, Varsha Singh¹, Evan Macosko², Sarah E. Steele¹, Cornelia I. Bargmann², and Alejandro Aballay¹

¹ Department of Molecular Genetics and Microbiology, Duke University Medical Center, Durham, North Carolina USA

² Howard Hughes Medical Institute and Laboratory of Neural Circuits and Behavior, The Rockefeller University, New York, New York USA

Abstract

A large body of evidence indicates that metazoan innate immunity is regulated by the nervous system, but the mechanisms involved in the process and the biological significance of such control remain unclear. We show that a neural circuit involving *npr-1*, which encodes a G-protein-coupled receptor related to mammalian neuropeptide Y receptors, functions to suppress innate immune responses. The inhibitory function of NPR-1 requires a cyclic GMP-gated ion channel encoded by *tax-2* and *tax-4* as well as the soluble guanylate cyclase GCY-35. Furthermore, we show that *npr-1*- and *gcy-35*-expressing sensory neurons actively suppress immune responses of non-neuronal tissues. A full-genome microarray analysis on animals with altered neural function due to mutation in *npr-1* shows an enrichment in genes that are markers of innate immune responses, including those regulated by a conserved PMK-1/P38 MAPK signaling pathway. These results present evidence that neurons directly control innate immunity in *C. elegans*, suggesting that G-protein coupled receptors may participate in neural circuits that receive inputs from either pathogens or infected sites and integrate them to coordinate appropriate immune responses.

Innate immune defense comprises a variety of mechanisms used by metazoans to prevent microbial infections. Activation of the innate immune system upon pathogen recognition results in a rapid and definitive microbicidal response to invading microorganisms that is fine-tuned to prevent deleterious deficiencies or excesses in the response. The nervous system, which can respond in milliseconds to many types of nonspecific environmental stimuli, has several characteristics that make it an ideal partner with the innate immune system to regulate nonspecific host defenses (1–3). However, even though a large body of evidence indicates that metazoan innate immunity is under the control of the nervous system, the mechanisms involved in the process and the biological significance of such control remain unclear. To provide insights into the neural mechanisms that regulate innate immunity, we have taken advantage of the simple and well studied nervous and innate immune systems of *Caenorhabditis elegans*.

The powerful genetic approaches available to *C. elegans* research have been used to address central questions concerning the functions of the nervous system (4). With its 302 neurons and 56 glial cells, which represent 37% of all somatic cells in a hermaphrodite, the nervous system is perhaps the most complex organ of *C. elegans*. Ablation of different neurons has demonstrated that sensory neurons regulate a variety of physiological processes, including dauer formation and adult lifespan (5–8). In addition, *C. elegans* neurons are known to express

*Corresponding author: a.aballay@duke.edu; FAX 919-684-2790.

numerous secreted peptides of the TGF beta family, the insulin family, and neuropeptide families (6,9–13). This myriad of secreted factors has the potential to act at a distance to modulate various physiological processes by regulating the function of neuronal and non-neuronal cells throughout the animal.

Like other free-living nematodes, *C. elegans* lives in soil environments where it is in contact with soil-borne microbes, including human microbial pathogens; it has evolved physiological mechanisms to respond to different pathogens by activating the expression of innate immune response genes that are conserved across metazoans (14–19). *C. elegans* also has behavioral responses to pathogenic bacteria such as *Bacillus thuringiensis* (20,21), *Microbacterium nematophilum* (22), *Photorhabdus luminescens* (23), *Pseudomonas aeruginosa* (24–26) and *Serratia marcescens* (24,27,28). Animals infected with these pathogens avoid lawns of the pathogen, or migrate away from pathogen odors. It is currently unknown how the nematode can sense pathogenic bacteria, though mutants in sensory transduction molecules such as the Gi-like protein ODR-3 and the G protein receptor kinase GRK-2 are incapable of *S. marcescens* lawn avoidance (28). These results suggest that G-protein coupled receptors may participate in neural circuits that receive inputs from either pathogens or infected sites and integrate them to coordinate appropriate defense responses.

To study the role of GPCRs in the regulation of innate immune response, we first determined the susceptibility of forty *C. elegans* strains carrying mutations in GPCRs to the human opportunistic pathogen *Pseudomonas aeruginosa* strain PA14, a clinical isolate capable of rapidly killing *C. elegans* at 25°C (29,30) (Table 1). Out of the 40 mutants studied, three mutants exhibited enhanced resistance to *P. aeruginosa* and only one mutant exhibited enhanced susceptibility to *P. aeruginosa* (Fig. 1, A and B). Interestingly, the strain exhibiting enhanced susceptibility to *P. aeruginosa*-mediated killing carries a loss-of-function mutation in *npr-1*, which encodes a G protein-coupled receptor related to mammalian neuropeptide Y receptors (31).

In order to determine whether the enhanced susceptibility to *P. aeruginosa* exhibited by *npr-1(ad609)* animals (Fig. 1A) was due to a reduction in lifespan or a deficient response to potentially pathogenic bacteria, *npr-1(ad609)* nematodes were fed heat-killed *P. aeruginosa* on plates supplemented with ampicillin. No difference in survival was seen between *npr-1(ad609)* and wild-type nematodes under these conditions, suggesting that the *npr-1* mutation affects the immune response to living pathogenic bacteria without altering the basic lifespan of the animals (Fig. 1C and Fig. S1).

We confirmed that NPR-1 is required for *C. elegans* defense to *P. aeruginosa* by exposing five additional *npr-1* mutants to the pathogen and comparing their survival to that of wild-type animals (Fig. 1D). Strains carrying loss-of-function alleles *npr-1(ky13)*, *npr-1(n1353)*, or *npr-1(ur89)* or the reduced-function allele *npr-1(g320)* were more susceptible to *P. aeruginosa* than wild-type, confirming that NPR-1 is required for the defense response to this pathogen. Interestingly, while the German wild isolate RC301, which contains the *npr-1(g320)* allele (31), is not significantly susceptible to *P. aeruginosa* compared to wild type, the *npr-1(g320)* allele confers susceptibility to *P. aeruginosa* in an N2 background (Fig. 1D). These results suggest that the German isolate may have evolved a mechanism to compensate for the increased susceptibility to pathogens due to reduced NPR-1 activity.

To determine whether the immune deficiency due to mutation in the *npr-1* gene is specific for *P. aeruginosa* infection, we exposed *npr-1(ad609)* nematodes to *Salmonella enterica* and *Enterococcus faecalis*, two human pathogens known to kill *C. elegans* (32–34). As shown in Figures S3A and S3B, *npr-1(ad609)* nematodes exhibited enhanced susceptibility to these pathogens, suggesting that NPR-1 is required for immune responses to pathogens in general.

NPR-1 is involved in a neural circuit that integrates behavioral responses to environmental oxygen, food, and other animals. In nature, NPR-1 is found in two allelic forms that differ in a single amino acid at position 215, NPR-1(215V) and NPR-1(215F) (31). The NPR1(215V) allele, which is found in the standard laboratory strain, has high activity whereas the NPR-1(215F) allele has low activity (35,36). Wild-type *npr-1(215V)* animals avoid oxygen levels above 10% when food is absent, but fail to avoid high oxygen in the presence of *E. coli* bacteria, the food provided to *C. elegans* in the laboratory. By contrast, *npr-1(215F)* and *npr-1* animals carrying loss-of-function (*lf*) alleles have strong hyperoxia avoidance in the absence or presence of *E. coli* (37). As a result, *npr-1(215F)* and *npr-1(lf)* show a preference for the thickest part of a bacterial lawn, the region in which oxygen levels are the lowest (35). In addition, as nematode aggregation into feeding groups decreases local oxygen concentrations, *npr-1(215F)* and *npr-1(lf)* form aggregates of nematodes when the animals are grown at densities high enough to allow this behavioral response (37).

One potential explanation for the reduced lifespan of *npr-1(lf)* mutants grown on bacterial pathogens is that aggregation increases nematode susceptibility to pathogen infection. However, the animal density in the assays where the susceptibility to pathogens is tested was not sufficient to elicit aggregation, making this possibility unlikely (Fig. 2D). Even though *npr-1(ad609)* animals did not aggregate, they still exhibited a preference for the thickest part of the lawn where oxygen concentrations are lower (Fig. 2, C and D). In addition, long-term exposure to *P. aeruginosa* caused wild-type animals to leave the bacterial lawn, a potentially protective behavioral response, but leaving was not observed in *npr-1(ad609)* animals. Although the number of bacterial cells in *npr-1(ad609)* animals was not found to be greater than that in wild-type animals (Fig. S2) at early stages of the infection, suggesting that the bacterial dose received by the two animals is comparable, we asked whether the behavior of *npr-1(ad609)* animals could affect susceptibility to pathogens. Thus, we grew animals on agar plates that were completely covered in *P. aeruginosa*, a condition that eliminates both the lawn border (favored by *npr-1* animals) and the ability to leave the lawn (favored by wild-type animals). As shown in Figure 2E, wild-type animals grown on plates completely covered by *P. aeruginosa* died at a higher rate than animals grown on plates containing a small lawn of *P. aeruginosa* in the center of the plate. *npr-1(ad609)* animals were equally susceptible to *P. aeruginosa* when grown on full or center lawns. Together, these results indicate that the lawn-leaving behavior of wild-type animals contributes to their increased survival. However, *npr-1(ad609)* animals still exhibited enhanced susceptibility to *P. aeruginosa* compared to wild type when the infections were performed in plates containing full lawns (Fig. 2E). These results indicate that lawn avoidance is part of *C. elegans* defense response to *P. aeruginosa*, but cannot account for all of the difference between wild-type and *npr-1(ad609)* animals.

To ask whether other elements of the oxygen response contribute to the enhanced susceptibility of *npr-1(ad609)* nematodes, animals grown at 21% oxygen were compared to those grown at 8% oxygen, a favorable oxygen environment that suppresses most behavioral phenotypes of *npr-1* mutants. Under 8% oxygen, *npr-1(ad609)* animals do not exhibit a preference for the bacterial border, and are capable of leaving the *P. aeruginosa* lawn. As shown in Figure 2F, *npr-1(ad609)* animals were more resistant to *P. aeruginosa*-mediated killing at 8% oxygen than at 21% oxygen, but were still more susceptible than wild-type animals at 8% oxygen. These results indicate that animals deficient in NPR-1 activity are more susceptible to *P. aeruginosa* due to two factors: decreased pathogen avoidance and decreased innate immune responses.

The increased susceptibility of *npr-1(ad609)* to *S. enterica* (Fig. S3A), a pathogen that does not elicit an avoidance behavior (38), is consistent with a role of NPR-1 in the regulation of immune responses that are independent of pathogen avoidance. Since a small amount of *S. enterica* that passes through the pharyngeal grinder proliferates and colonizes the intestine in

a process that is independent of the dose (32), and the pumping rates of *npr-1(ad609)* animals are comparable to those of wild type (Fig. S4), the results further support the function of NPR-1 in the regulation on immune responses.

Genetic studies have identified a chemosensory circuit that coordinates oxygen preference and aggregation in *npr-1* mutants (35,37,39–42). Aggregation and bordering of *npr-1(ad609)* nematodes depend on functional *gcy-35*, *tax-2*, or *tax-4* genes (31,40,43). GCY-35 is a soluble guanylyl cyclase (sGC) that binds directly to molecular oxygen, and TAX-2 and TAX-4 are two subunits of a cGMP-gated-ion-channel (31,40,43). Through the activity of GCY-35 and other guanylate cyclases and the subsequent activation of TAX-2/TAX-4, AQR, PQR, and URX sensory neurons drive avoidance of high oxygen; these neurons are thought to be hyperactive in *npr-1* mutants (40). To determine whether this part of the NPR-1 neural circuit regulates innate immune response, we studied the pathogen susceptibility of *npr-1(ad609)* animals carrying loss-of-function mutations in *gcy-35*, *tax-2*, or *tax-4*. As shown in Figure 3, the enhanced susceptibility to *P. aeruginosa* of *npr-1(ad609)* animals was rescued by mutations in *gcy-35*, *tax-2*, or *tax-4*. Similar results were obtained when the infections were performed in plates containing full lawns of *P. aeruginosa* (Fig. S5).

NPR-1 is expressed in at least twenty different neurons, including the *gcy-35*-expressing sensory neurons AQR, PQR, and URX (35). To confirm that at least AQR, PQR, and URX neurons are part of a neural network that inhibits innate immunity, we studied the susceptibility to *P. aeruginosa* of a strain in which these neurons were genetically ablated by expressing the cell-death activator gene *egl-1* under the control of the *gcy-36* promoter (42). The strain lacking AQR, PQR and URX neurons exhibited a significantly increased survival on *P. aeruginosa* (Fig. 3D), indicating that AQR, PQR and URX neurons suppress innate immunity. In addition, lack of AQR, PQR and URX neurons partially rescued the enhanced susceptibility to *P. aeruginosa* of *npr-1(ad609)* animals (Fig. 3D). Expression of *npr-1* under the control of the *gcy-32* promoter, which drives the expression of *npr-1* to AQR, PQR and URX neurons, also rescued the enhanced susceptibility to *P. aeruginosa* of *npr-1(ad609)* animals (Fig. 3E), providing additional support to the role of these neurons in the regulation of innate immunity. Consistent with the idea that additional NPR-1 expressing neurons regulate innate immunity (Fig. 3F), *npr-1* expression under the regulation of its own promoter fully rescued the enhanced susceptibility to *P. aeruginosa* phenotype of *npr-1(ad609)* animals (Fig. 3E). Taken together, these results indicate that genes and cells involved in the NPR-1 neural circuit modulate innate immune responses.

As in mammals, peristalsis, low pH, and antimicrobial substances prevent microbial colonization of the *C. elegans* intestine. In addition, accumulating evidence indicates that different genetic pathways regulate the expression of *C. elegans* genes that are markers of immune response (14–19). To provide insight into the immune function of the NPR-1 neural circuit, we utilized gene expression microarrays to find clusters of genes upregulated or downregulated in *npr-1(ad609)* mutants relative to wild-type animals grown on live *P. aeruginosa* (Tables 2 and 3). Interestingly, there is a significant enrichment in NPR-1-regulated genes that have at least one of three features: they are upregulated by *P. aeruginosa* infection in wild-type animals, expressed in the intestine, and/or have already been linked to the *C. elegans* P38 MAP kinase, PMK-1, which plays a crucial role in innate immunity (17,44–47) (Table 4). Further analysis revealed that five of the genes most highly downregulated by NPR-1 are found in a cluster on chromosome V that appears to have been duplicated further downstream on that chromosome (Table 3). Of these five genes, three are also known to be downregulated by the *C. elegans* PMK-1/P38 pathway. Overall, most of the genes regulated by pathways linked to innate immunity correspond to PMK-1-regulated genes (Fig. 4K). In addition, these genes are similarly misregulated in animals deficient in NPR-1 or PMK-1 function (Tables 2 and 3). Since *pmk-1* is not transcriptionally regulated by NPR-1 (Tables 2

and 3), we studied whether NPR-1 regulates PMK-1 at the post-transcriptional level. As shown in Figure 4L, *npr-1(ad609)* nematodes exhibit lower levels of active PMK-1 than wild-type nematodes, suggesting that the NPR-1 neural circuit modulates the activation of PMK-1. Inhibition of *pmk-1* gene expression by RNAi in *npr-1(ad609)* nematodes results in increased susceptibility (Fig. S6), indicating that while the NPR-1 mediated immune pathway has overlapping targets with the PMK-1 mediated immune pathway, NPR-1 regulates both PMK-1-dependent and independent immune responses.

To obtain insight into the mechanism by which *gcy-35* mutation rescues the enhanced susceptibility to *P. aeruginosa* of *npr-1(ad609)* animals (Fig. 3A), we used quantitative RT-PCR (qRT-PCR) to compare the expression levels of selected genes of *npr-1(ad609)* to that of *npr-1(ad609);gcy-35(ok769)* animals. As shown in Figure 4, a *gcy-35* mutation in *npr-1(ad609)* animals rescues the altered expression of 10 out of 19 genes tested that are markers of *C. elegans* immune response. These results indicate that the NPR-1 neural circuit modulates the expression of immune-related genes, many of which are known to be expressed in tissues that are in direct contact with pathogens during infection.

In summary, our results provide evidence that specific genes and neurons in the nervous system are responsible for effective innate immune responses that are independent of behavioral phenotypes and may take place in tissues that are in direct contact with pathogens. It has recently been postulated that cell non-autonomous signals from different neurons may act on non-neural tissues to regulate processes such as fat storage (48) and longevity (8). *C. elegans* neurons can regulate physiological processes through conserved neuroendocrine signals including insulin-related peptides, TGF-beta peptides, and neuropeptides. The URX, AQR, and PQR neurons that are part of the NPR-1 neural circuit that regulates innate immunity are exposed to the pseudocoelomic body fluid, which could communicate neuroendocrine signals to non-neural tissues involved in defense responses. The identification and characterization of the specific neuroendocrine signals that regulate innate immune responses in *C. elegans* should yield significant insights into the mechanisms used by the nervous system to regulate similar processes across metazoans.

Supplementary Material

Refer to Web version on PubMed Central for supplementary material.

Acknowledgments

We thank *Caenorhabditis* Genetics Center (University of Minnesota) for strains used in this study. A.A. is funded by The Whitehead Scholars Program, NIH SERCEB (U54 AI057157), and NIH GM070977.

References

1. Sternberg EM. Nat Rev Immunol Apr;2006 6:318. [PubMed: 16557263]
2. Andersson J. J Intern Med Feb;2005 257:122. [PubMed: 15656871]
3. Tracey KJ. Nature Dec 19–26;2002 420:853. [PubMed: 12490958]
4. Sattelle DB, Buckingham SD. Invert Neurosci Mar;2006 6:1. [PubMed: 16470388]
5. Bargmann CI, Horvitz HR. Science Mar 8;1991 251:1243. [PubMed: 2006412]
6. Schackwitz WS, Inoue T, Thomas JH. Neuron Oct;1996 17:719. [PubMed: 8893028]
7. Alcedo J, Kenyon C. Neuron Jan 8;2004 41:45. [PubMed: 14715134]
8. Bishop NA, Guarente L. Nature May 31;2007 447:545. [PubMed: 17538612]
9. Li C, Nelson LS, Kim K, Nathoo A, Hart AC. Ann N Y Acad Sci 1999;897:239. [PubMed: 10676452]
10. Li W, Kennedy SG, Ruvkun G. Genes Dev Apr 1;2003 17:844. [PubMed: 12654727]

11. Nathoo AN, Moeller RA, Westlund BA, Hart AC. *Proc Natl Acad Sci U S A* Nov 20;2001 98:14000. [PubMed: 11717458]
12. Pierce SB, et al. *Genes Dev* Mar 15;2001 15:672. [PubMed: 11274053]
13. Ren P, et al. *Science* Nov 22;1996 274:1389. [PubMed: 8910282]
14. Mallo GV, et al. *Curr Biol* 2002;12:1209. [PubMed: 12176330]
15. Kerry S, Tekippe M, Gaddis NC, Aballay A. *PLoS ONE* Dec 20;2006 1:e77. [PubMed: 17183709]
16. Shapira M, et al. *Proc Natl Acad Sci U S A* Sep 19;2006 103:14086. [PubMed: 16968778]
17. Troemel ER, et al. *PLoS Genet* Nov 10;2006 :2.
18. Wong D, Bazopoulou D, Pujol N, Tavernarakis N, Ewbank JJ. *Genome Biol* Sep 17;2007 8:R194. [PubMed: 17875205]
19. O'Rourke D, Baban D, Demidova M, Mott R, Hodgkin J. *Genome Res* Aug;2006 16:1005. [PubMed: 16809667]
20. Schulenburg H, Muller S. *Parasitology* Apr;2004 128:433. [PubMed: 15151149]
21. Hasshoff M, Bohnisch C, Tonn D, Hasert B, Schulenburg H. *Faseb J* Jun;2007 21:1801. [PubMed: 17314144]
22. Yook K, Hodgkin J. *Genetics* Feb;2007 175:681. [PubMed: 17151260]
23. Sicard M, Hering S, Schulte R, Gaudriault S, Schulenburg H. *Environ Microbiol* Jan;2007 9:12. [PubMed: 17227408]
24. Zhang Y, Lu H, Bargmann CI. *Nature* Nov 10;2005 438:179. [PubMed: 16281027]
25. Beale E, Li G, Tan MW, Rumbaugh KP. *Appl Environ Microbiol* Jul;2006 72:5135. [PubMed: 16820523]
26. Laws TR, Atkins HS, Atkins TP, Titball RW. *Microb Pathog* Jun;2006 40:293. [PubMed: 16678995]
27. Pujol N, et al. *Curr Biol* 2001;11:809. [PubMed: 11516642]
28. Pradel E, et al. *Proc Natl Acad Sci U S A* Feb 13;2007 104:2295. [PubMed: 17267603]
29. Tan MW, Mahajan-Miklos S, Ausubel FM. *Proc Natl Acad Sci U S A* 1999;96:715. [PubMed: 9892699]
30. Mahajan-Miklos S, Tan MW, Rahme LG, Ausubel FM. *Cell* 1999;96:47. [PubMed: 9989496]
31. de Bono M, Bargmann CI. *Cell* Sep 4;1998 94:679. [PubMed: 9741632]
32. Aballay A, Yorgey P, Ausubel FM. *Curr Biol* 2000;10:1539. [PubMed: 11114525]
33. Labrousse A, Chauvet S, Couillault C, Kurz CL, Ewbank JJ. *Curr Biol* 2000;10:1543. [PubMed: 11114526]
34. Garsin DA, et al. *Proc Natl Acad Sci U S A* 2001;98:10892. [PubMed: 11535834]
35. Coates JC, de Bono M. *Nature* Oct 31;2002 419:925. [PubMed: 12410311]
36. Rogers C, et al. *Nat Neurosci* Nov;2003 6:1178. [PubMed: 14555955]
37. Gray JM, et al. *Nature* Jul 15;2004 430:317. [PubMed: 15220933]
38. Tenor JL, Aballay A. *EMBO Rep* Jan;2008 9:103. [PubMed: 17975555]
39. de Bono M, Tobin DM, Davis MW, Avery L, Bargmann CI. *Nature* Oct 31;2002 419:899. [PubMed: 12410303]
40. Cheung BH, Cohen M, Rogers C, Albayram O, de Bono M. *Curr Biol* May 24;2005 15:905. [PubMed: 15916947]
41. Rogers C, Persson A, Cheung B, de Bono M. *Curr Biol* Apr 4;2006 16:649. [PubMed: 16581509]
42. Chang AJ, Chronis N, Karow DS, Marletta MA, Bargmann CI. *PLoS Biol* Sep;2006 4:e274. [PubMed: 16903785]
43. Cheung BH, Arellano-Carbajal F, Rybicki I, de Bono M. *Curr Biol* Jun 22;2004 14:1105. [PubMed: 15203005]
44. Kim DH, et al. *Science* 2002;297:623. [PubMed: 12142542]
45. Aballay A, Drenkard E, Hilbun LR, Ausubel FM. *Curr Biol* 2003;13:47. [PubMed: 12526744]
46. Kim DH, et al. *Proc Natl Acad Sci U S A* Jul 27;2004 101:10990. [PubMed: 15256594]
47. Huffman DL, et al. *Proc Natl Acad Sci U S A* Jul 27;2004 101:10995. [PubMed: 15256590]
48. Mak HY, Nelson LS, Basson M, Johnson CD, Ruvkun G. *Nat Genet* Mar;2006 38:363. [PubMed: 16462744]

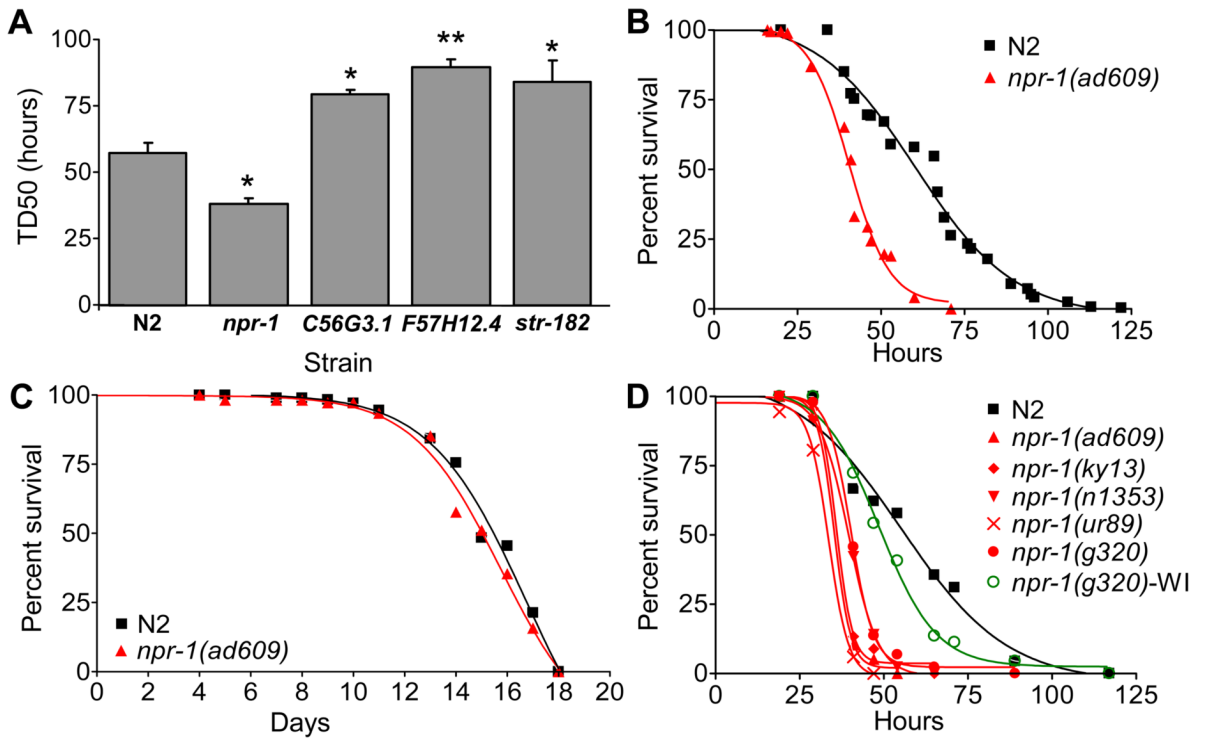


Fig. 1. *C. elegans* G-protein coupled receptor NPR-1 is involved in immunity to *P. aeruginosa*. (A) *C. elegans* strains carrying mutations in GPCRs were screened for altered survival on *P. aeruginosa*. *C56G3.1(ok1439)* (P=0.0347), *F57H12.4(ok1504)* (P=0.0071), and *str-182(ok1419)* (P=0.0342) had enhanced resistance to *P. aeruginosa* and *npr-1(ad609)* (P=0.0246) had enhanced susceptibility to *P. aeruginosa*. Shown is the time required for 50% of the nematodes to die (TD₅₀) as mean ± SEM corresponding to at least three independent experiments, each of which used at least 40 adult nematodes per strain. (B) Wild-type N2 and *npr-1(ad609)* (P=0.0001) nematodes were exposed to *P. aeruginosa* and scored for survival over time. The graph represents combined results of four independent experiments, N≥40 adult nematodes per strain. (C) Wild-type N2 and *npr-1(ad609)* (P=0.1411) nematodes were exposed to heat-killed *P. aeruginosa* and scored for survival over time. The graph represents the combined results of two independent experiments, N=100 adult nematodes per strain. (D) Wild-type N2, *npr-1(ad609)* (P=0.0001), *npr-1(ky13)* (P=0.0001), *npr-1(n1353)* (P=0.0001), *npr-1(ur89)* (P=0.0001), *npr-1(g320)* (P=0.0001), and the wild isolate (WI) *npr-1(g320)* (P=0.0922) were exposed to *P. aeruginosa* and scored for survival over time. Shown is a representative assay of at least 3 independent experiments, N=48 adult nematodes per strain.

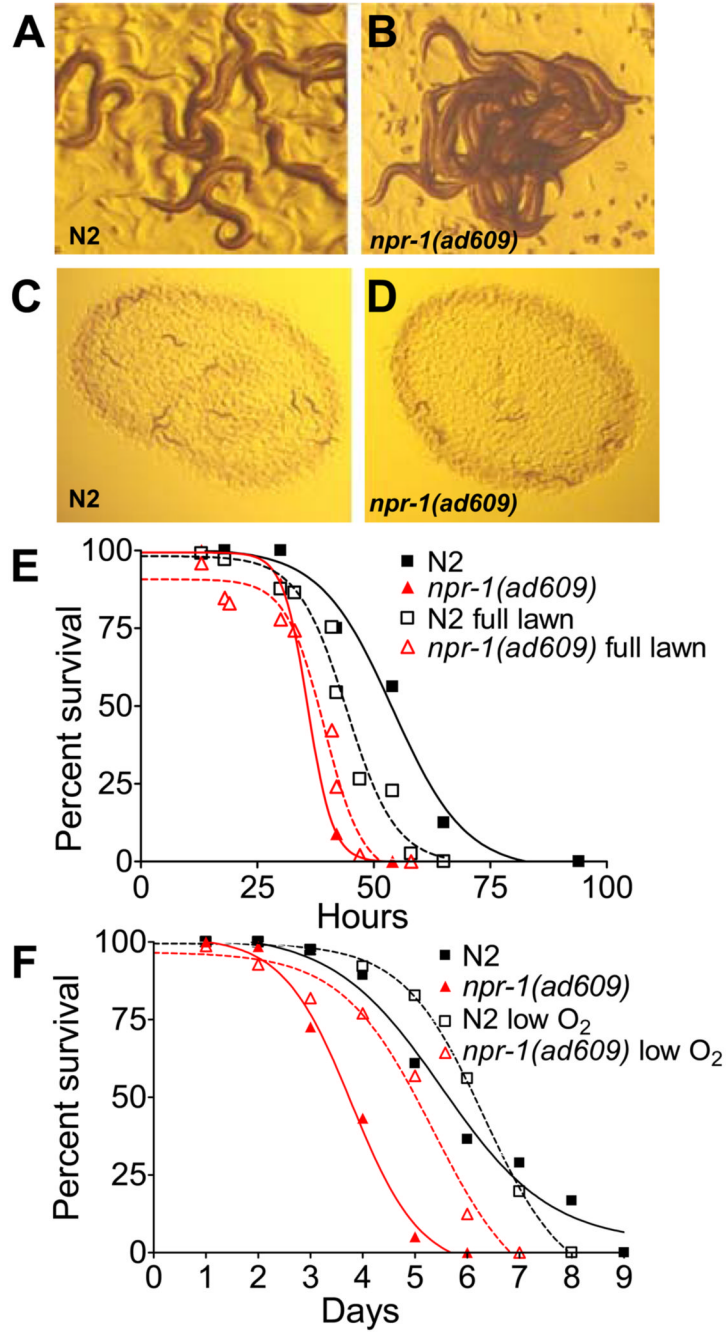


Fig. 2. Hyperoxia avoidance of NPR-1-deficient animals increases susceptibility to *P. aeruginosa*. (A) *C. elegans* wild-type N2 animals and (B) *npr-1(ad609)* mutants were propagated at 20°C as hermaphrodites on modified NG agar plates seeded with *E. coli* strain OP50 and then visualized using a Leica MZ FLIII stereomicroscope. The characteristic aggregate of *npr-1(ad609)* nematodes shown here is at the edge of the bacterial lawn. (C) Twelve wild-type N2 and (D) twelve *npr-1(ad609)* nematodes were exposed to *P. aeruginosa* for 24 hours under standard killing assay conditions and visualized using a Leica MZ FLIII stereomicroscope. Under these conditions, *npr-1(ad609)* nematodes do not form characteristic aggregates of the strain. (E) Wild-type N2 and *npr-1(ad609)* nematodes were exposed to either a full lawn or a

center lawn of *P. aeruginosa* on a 3.5 cm in diameter plate and scored for survival over time. Under both conditions *npr-1(ad609)* animals were more susceptible to *P. aeruginosa*-mediated killing ($P=0.0001$). Wild-type animals on full lawns were more susceptible to *P. aeruginosa*-mediated killing than animals on center lawns ($P=0.0001$); *npr-1(ad609)* animals were equally susceptible ($P=0.07$). The graph represents combined results of three independent experiments, $N \geq 40$ adult nematodes per strain. (F) Wild-type N2 and *npr-1(ad609)* nematodes at exposed to *P. aeruginosa* at either 21% or 8% oxygen and scored for survival over time. Under both conditions *npr-1(ad609)* animals were more susceptible to *P. aeruginosa*-mediated killing ($P=0.0001$). *npr-1(ad609)* animals at 21% oxygen were more susceptible to *P. aeruginosa*-mediated killing than animals at 8% oxygen ($P=0.0001$); wild-type animals were equally susceptible ($P=0.95$). The graph represents combined results of two independent experiments, $N=40$ adult nematodes per strain.

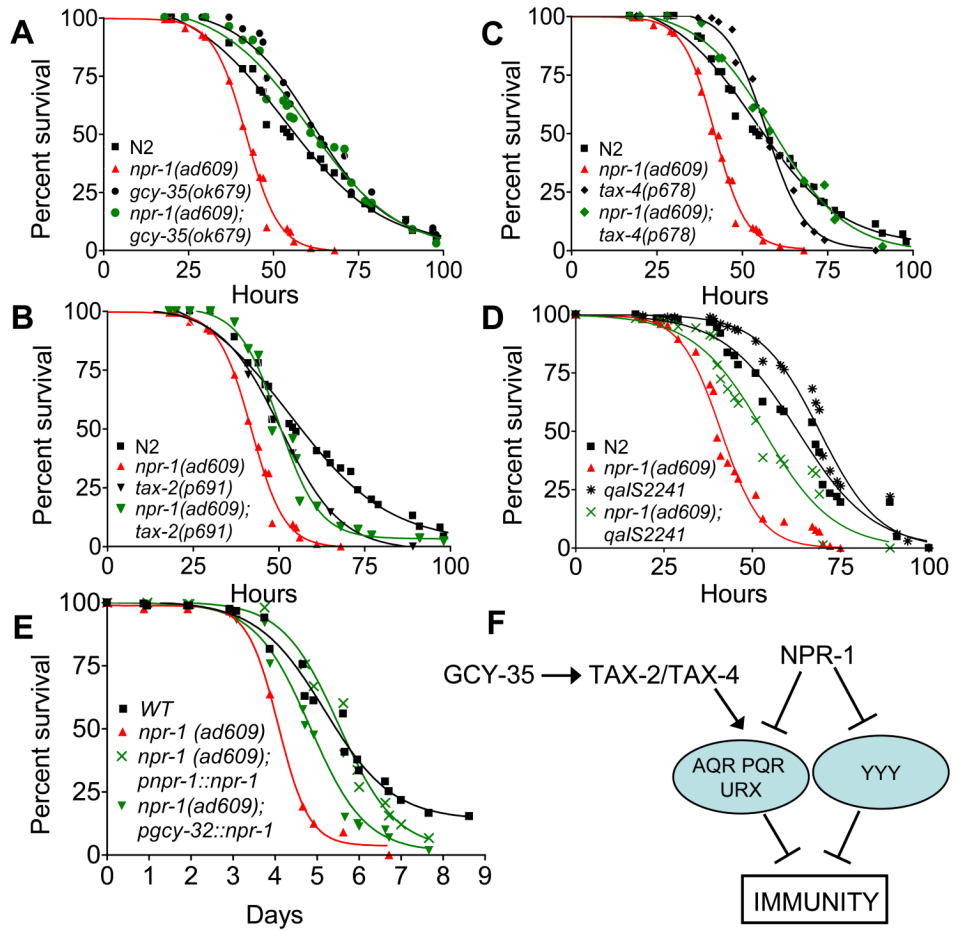


Fig. 3. The NPR-1 neural circuit regulates innate immunity. (A) Wild-type N2, *npr-1(ad609)* ($P=0.0001$), *gcy-35(ok769)* ($P=0.0125$), and *gcy-35(ok769);npr-1(ad609)* ($P=0.0639$) were exposed to *P. aeruginosa*. (B) Wild-type N2, *npr-1(ad609)* ($P=0.0001$), *tax-4(p678)* ($P=0.1673$), *tax-4(p678);npr-1(ad609)* ($P=0.3611$), were exposed to *P. aeruginosa*. (C) Wild-type N2, *npr-1(ad609)* ($P=0.0001$), *tax-2(p691)* ($P=0.0930$), *tax-2(p691);npr-1(ad609)* ($P=0.0031$) were exposed to *P. aeruginosa*. (D) Wild-type N2, *npr-1(ad609)* ($P=0.0001$), *qalS2241* ($P=0.0042$), a strain which lacks AQR, PQR, and URX neurons, and *npr-1(ad609);qalS2241* ($P=0.0001$) were exposed to *P. aeruginosa*. The graphs represent combined results of at least three independent experiments, $N \geq 40$ adult nematodes per strain. (E) Wild-type N2, *npr-1(ad609)* ($P=0.0001$), *pgcy-32::npr-1*; *npr-1(ad609)* ($P=0.0001$), and *pnpr-1::npr-1*; *npr-1(ad609)* ($P=0.1939$) were exposed to *P. aeruginosa*. The graphs represent combined results of at least two independent experiments, $N \geq 100$ adult nematodes per strain. Killing assays were performed at 17°C, as low temperatures are known to increase the resolution of killing assays involving *P. aeruginosa*. (F) Model of the neural control of innate immunity in *C. elegans*: NPR-1 inhibits the activity of AQR, PQR, URX and additional neuron(s) designated YYY that suppress innate immunity, while GCY-35, TAX-2, and TAX-4 are required for the activation of AQR, PQR and URX neurons.

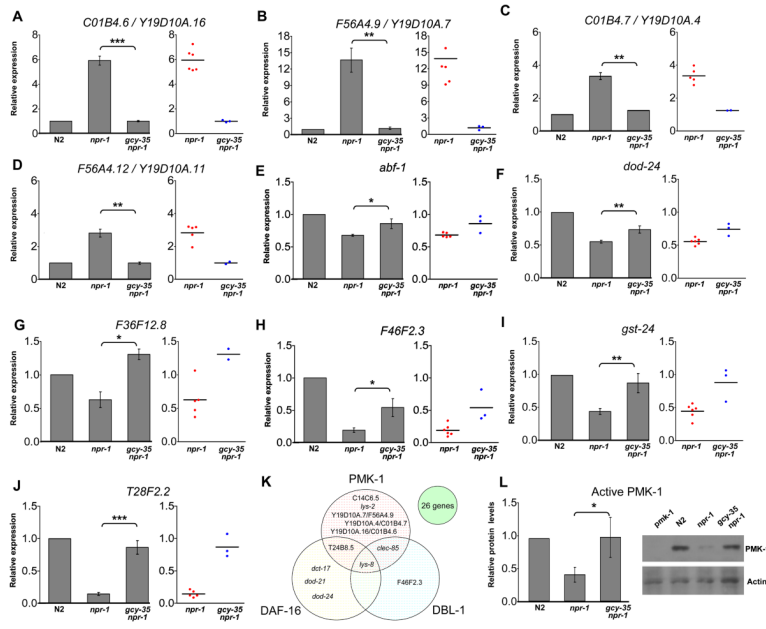


Fig. 4. The NPR-1 neural circuit regulates expression of innate immune genes. (A–J) Quantitative reverse transcription–PCR analysis of *C01B4.6/Y19D10A.16*, *F56A4.9/Y19D10A.7*, *C01B4.7/Y19D10A.4*, *F56A4.12/Y19D10A.11*, *abf-1*, *dod-24*, *F36F12.8*, *F46F2.3*, *gst-24*, and *T28F2.2* expression in *npr-1(ad609)* and *gcy-35(ok769);npr-1(ad609)* nematodes relative to wild-type nematodes exposed to *P. aeruginosa*. Data were analyzed by normalization to pan-actin (*act-1,-3,-4*) and relative quantification using the comparative cycle threshold method. Student’s exact *t*-test indicates differences among the groups are significantly different; bar graphs correspond to mean \pm SEM. Point graphs correspond to gene quantification in independent isolations of *npr-1(ad609)*(N=6) and *gcy-35(ok769);npr-1(ad609)*(N=3). (K) The Venn diagram lists the genes identified by microarray analysis to be regulated by both NPR-1 and one or more known innate immune pathways in *C. elegans*. Genes that lie within two or three circles are regulated by multiple innate immune pathways in addition to NPR-1. Twenty-six genes have not been previously connected to any of the innate immune pathways and are depicted in the solitary circle. (L) Immunological detection of active PMK-1. Active PMK-1 was detected in wild-type N2, *npr-1(ad609)* and *gcy-35(ok769);npr-1(ad609)*. Animals were grown at 20°C until 1 day old adult and whole worm lysates were used to detect active PMK-1 by Western blotting using an anti-human p38 antibody from Promega, Inc. Actin was detected using a polyclonal antibody from SIGMA. BioRad Quantity One Analysis Software was used to scan and analyze the Western blot.

Table 1

GPCRs are involved in innate immunity to *P. aeruginosa*

Strain	Gene	Description	Closest human homolog ^a	Expression Pattern	TD50 Mean±SEM, N	P-value	PA14 phenotype ^b
N2	---	---	---	---	57.20 ± 5.748 N=5	---	WT
RB799	<i>C25G6.5</i>	Putative GPCR	Prolactin-releasing peptide receptor	AIA, AIY, PVQ	68.00 ± 5.115 N=4	0.2147	WT
RB1284	<i>C30F12.6</i>	Putative GPCR	Thyrotropin-releasing hormone receptor	pharynx, intestine	68.33 ± 5.925 N=3	0.2528	WT
RB1289	<i>C43C3.2</i>	Putative GPCR	Melanin-concentrating hormone receptor 1	unknown	68.00 ± 7.000 N=2	0.3427	WT
RB1288	<i>C48C5.1</i>	Putative GPCR	Neurotrophin U receptor 2	unknown	81.50 ± 9.500 N=2	0.0753	ERP
RB1423	<i>C49A9.7</i>	Putative GPCR	Substance P receptor	unknown	70.00 ± 7.572 N=3	0.2244	WT
RB1321	<i>C56G3.1</i>	Putative GPCR	Isoform B of Somatostatin receptor	unknown	78.33 ± 1.764 N=3	0.0347*	ERP
RB1162	<i>cfz-2</i>	Frizzled family of membrane receptors	Frizzled-8 precursor	pharyngeal neurons	51.25 ± 4.820 N=4	0.4689	WT
RB665	<i>dop-1</i>	D1-like dopamine receptor	D(1B) dopamine receptor	head support cells, RIS, AVM, ALM, ALN, PLN, PVQ, PLM, PHC, ALM, AUA, RIB, RIM	68.75 ± 3.945 N=4	0.1616	WT
LX702	<i>dop-2</i>	D2-like dopamine receptor	Isoform 3 of D(2) dopamine receptor	RIA, SIA, SIB, RID, PDA	55.00 ± 3.606 N=3	0.7951	WT
BZ873	<i>dop-3</i>	D2-like dopamine receptor	Isoform 2 of D(2) dopamine receptor	neurons of the head, ventral cord and tail, GABAergic neurons	39.50 ± 0.5000 N=2	0.1252	ESP
RB761	<i>F35G8.1</i>	Putative GPCR	Isoform 2 of Neuropeptide FF receptor 2	unknown	60.00 ± 6.245 N=3	0.7642	WT
RB509	<i>gnrr-1</i>	GoNadotropin-Releasing hormone Receptor	Isoform 1 of Gonadotropin-releasing hormone receptor	unknown	74.33 ± 6.173 N=3	0.1023	WT
RB1349	<i>F57H12.4</i>	Putative GPCR	Isoform 1A of Growth hormone secretagogue receptor type 1	unknown	89.33 ± 3.283 N=3	0.0071**	ERP
RB896	<i>gar-1</i>	G-protein-linked acetylcholine receptor	Muscarinic acetylcholine receptor M1	ciliated head neurons, PVM	72.00 ± 4.000 N=3	0.1212	WT
RB756	<i>gar-2</i>	G-protein-linked acetylcholine receptor	Muscarinic acetylcholine receptor M2	sensory, ventral cord neurons, HSN	64.00 ± 5.033 N=3	0.4542	WT
JD217	<i>gar-3</i>	G-protein-linked acetylcholine receptor	Muscarinic acetylcholine receptor M1	pharyngeal muscle, I3, extrapharyngeal neurons	75.50 ± 7.500 N=2	0.1389	WT
VCI58	<i>lat-2</i>	Latrophilin receptor	Uncharacterized protein LPHN2	g1 gland cells, arcade cells	56.50 ± 3.279 N=4	0.9245	WT
DA609	<i>npr-1</i>	G-protein coupled neuropeptide receptor	Isoform 2 of Neuropeptide FF receptor 2	AQR, ASE, ASG, ASH, URX, IL2L/R, OLO, AUA, SAA, RMG, SMBD, M3,	37.80 ± 4.067 N=5	0.0246*	ESP

Strain	Gene	Description	Closest human homolog ^d	Expression Pattern VD, DD, PQR, PHA, PHB, RIV, RIG, SDQ	TD50 Mean±SEM, N	P-value	PA14 phenotype ^b
XA3702	<i>npr-2</i>	G-protein coupled neuropeptide receptor	Isoform 2 of Neuropeptide FF receptor 2	unknown	62.67 ± 2.186 N=3	0.5111	WT
CX3410	<i>odr-10</i>	Odorant receptor	Olfactory receptor 5B17	AWA	62.00 ± 2.517 N=3	0.5648	WT
RBI141	<i>R13H7.2</i>	Putative GPCR	Neuromedin U receptor 2	Intestine, head neurons	64.67 ± 2.028 N=3	0.3757	WT
DA1814	<i>ser-1</i>	Serotonin/octopamine receptor	5-hydroxytryptamine 2A receptor	RMH, RMF, RMD, pharyngeal muscles	63.00 ± 8.505 N=3	0.578	WT
OHS13	<i>ser-2</i>	Serotonin/octopamine receptor	5-hydroxytryptamine receptor 1A	AIY, AVH, AUA, RIC, SAB, RID, RIA, SDQ, CAN, DA9, LUA, ALN, PVC, NSM, AIZ, DVA, BDU, SIA, PVT, RME, OLL, PVD	54.00 ± 8.963 N=3	0.7616	WT
RBI1622	<i>ser-3</i>	Serotonin/octopamine receptor	Isoform 2 of Alpha-1A adrenergic receptor	Head, tail neurons	64.25 ± 4.956 N=4	0.3983	WT
AQ866	<i>ser-4</i>	Serotonin/octopamine receptor	5-hydroxytryptamine receptor 1B	PVT, RIB, DVA, RIS, DVC	59.00 ± 2.517 N=3	0.8269	WT
DA2100	<i>ser-7</i>	Serotonin/octopamine receptor	Isoform D of 5- hydroxytryptamine receptor 7	Pharyngeal neurons MC, M4, I2, I3, M5, M3, I4, I6 and M2	61.00 ± 2.000 N=3	0.6435	WT
CB5414	<i>srd-1</i>	Serpentine Receptor, class D	Melanin-concentrating hormone receptor 2	ASI	58.00 ± 2.082 N=3	0.9218	WT
VC459	<i>srd-2</i>	Serpentine Receptor, class D	G protein-coupled receptor MRGX1	unknown	62.67 ± 6.839 N=3	0.572	WT
RBI1526	<i>srd-44</i>	Serpentine Receptor, class D	DRG kappa 1 splice variant KOR 1A	unknown	59.00 ± 6.494 N=4	0.8413	WT
RBI1419	<i>snv-140</i>	Serpentine Receptor, class W	Isoform 1A of Growth hormone secretagogue receptor type 1	unknown	58.67 ± 8.192 N=3	0.885	WT
RBI306	<i>str-182</i>	7-transmembrane olfactory receptor	none	unknown	83.33 ± 7.860 N=3	0.0342*	ERP
VC342	<i>str-31</i>	7-transmembrane olfactory receptor	Frizzled-8 precursor	unknown	64.25 ± 6.945 N=4	0.4556	WT
RB785	<i>T02E9.3</i>	Putative GPCR	Isoform 2 of D(2) dopamine receptor	Head, tail neurons	57.00 ± 2.646 N=3	0.9806	WT
VC125	<i>tag-126</i>	Tyramine receptor	beta-1-adrenergic receptor	Head, tail neurons, vulva	68.67 ± 0.3333 N=3	0.1854	WT
VC224	<i>tag-24</i>	Biogenic amine receptor	Alpha-2A adrenergic receptor	Head, tail neurons	76.67 ± 6.839 N=3	0.0774	ERP
VC270	<i>tag-49</i>	Putative GPCR	Neuromedin-K receptor	Intestine, renal gland cells, nervous system	67.67 ± 5.840 N=3	0.2778	WT
VC273	<i>tag-89</i>	Putative GPCR	Thyrotropin-releasing hormone receptor	unknown	70.00 ± 3.937 N=4	0.1264	WT
RBI1365	<i>uvr-6</i>	Vitellogenin-linked GPCR	Somatostatin receptor type 3	Head, tail neurons, ventral nerve cord, anal depressor cell, VMI	53.33 ± 7.311 N=3	0.6933	WT
RBI1393	<i>Y58G8A.4</i>	Putative GPCR	Prolactin-releasing peptide receptor	unknown	59.00 ± 4.619 N=3	0.8369	WT

Strain	Gene	Description	Closest human homolog ^a	Expression Pattern	TD50 Mean±SEM, N	P-value	PA14 phenotype ^b
RB1405	<i>Y59H11A.L1</i>	Putative GPCR	Substance-K receptor	unknown	62.33 ± 1.202 N=3	0.5305	WT

^aBest BLASTP matches to longest protein product (www.wormbase.org)

^bERP: enhanced resistance to *P. aeruginosa*; ESP: enhanced susceptibility to *P. aeruginosa*; Strains were considered to be significantly different from wild-type using Student's exact t-test (bold). Additional strains are designated ERP or ESP due to significant differences ($p < 0.0001$) in survival compared to wild-type in two independent experiments using PRISM to apply a logrank test.

Genes upregulated by NPR-1

Table 2

Gene	Description	Intestinal expression ^d	↑ on PA14 ^b	Known immune pathway ^c	Microarray		qRT-PCR		<i>p</i> -value
					mean ± SEM ^d	mean ± SEM ^d	mean ± SEM ^d	mean ± SEM ^d	
<i>dct-17</i>	Germline tumor affecting		Y	daf-16	0.176±0.023	0.5411±0.0505	ND	0.0003	
<i>F15D4.5</i>	Similarity to human synaptonemal complex protein				0.303±0.029	ND			
<i>dod-21</i>	Lifespan abnormal (RNAi)			daf-16	0.3385±0.0325	0.4256±0.0775		0.0007	
<i>F36F12.8</i>	Zinc finger protein				0.3575±0.0115	0.6271±0.1184		0.0346	
<i>F46F2.3</i>	None	Y		dbl-1	0.364±0.054	0.1904±0.0356		0.0001	
<i>F13H8.3</i>	Predicted inosine-uridine nucleoside hydrolase				0.3845±0.0595	ND			
<i>gst-24</i>	Glutathione S-transferase	Y	Y		0.3945±0.0285	0.4442±0.0437		0.0001	
<i>stdh-2</i>	Steroid dehydrogenase, lifespan abnormal(RNAi)		Y		0.3995±0.0805	0.4456±0.0713		0.0015	
<i>T10D4.6</i>	None				0.4065±0.0505	ND			
<i>Y69A2AR.25</i>	Similarity to human neurogenic locus notch				0.4135±0.0345	ND			
<i>gst-20</i>	Glutathione S-transferase				0.4165±0.0405	ND			
<i>T24B8.5</i>	Similarity to roundworm mucin MUC-5		Y	daf-16, pmk-1	0.426±0.028	ND			
<i>T28F2.2</i>	Slow growth, decreased brood size (RNAi)	Y			0.4275±0.0045	0.1441±0.0231		0.0001	
<i>F36G9.12</i>	Predicted transcription factor, transferase activity		Y		0.436±0.027	ND			
<i>col-101</i>	Cuticle collagen				0.467±0.013	ND			
<i>C14C6.5</i>	None	Y	Y	pmk-1	0.468±0.008	0.5562±0.0869		0.0070	
<i>clcc-85</i>	C-type lectin	Y	Y	dbl-1, pmk-1	0.6025±0.0995	0.5661±0.0549		0.0042	
<i>dod-24</i>	CUB like region, lifespan abnormal (RNAi)		Y	daf-16	0.7555±0.0185	0.5546±0.0201		0.0001	
<i>lec-11</i>	Galectin family, binds sugar in vitro	Y	Y		0.7655±0.0875	0.6171±0.0401		0.0024	
<i>abf-1</i>	Antibacterial factor	Y	Y		0.8015±0.0225	0.682±0.0157		0.0001	
<i>lys-8</i>	Putative lysozyme, lifespan abnormal(RNAi)	Y	Y	daf-16, dbl-1, pmk-1	0.832±0.003	0.7331±0.0648		0.0092	

Gene	Description	Intestinal expression ^a	↑ on PA14 ^b	Known immune pathway ^c	Microarray		qRT-PCR		p-value
					mean ± SEM ^d	mean ± SEM ^d	mean ± SEM ^d	mean ± SEM ^d	
<i>lys-2</i>	Putative lysozyme	Y	Y	pmk-1	0.851±0.044	0.5561±0.0257			0.0004

^a Genes expressed in the intestine of *C. elegans* (6)

^b Genes upregulated in response to *P. aeruginosa* infection (7,8)

^c Genes previously linked to known innate immune pathways (8–11)

^d Expression level relative to wild-type

Table 3

Genes downregulated by NPR-1

Gene	Description	Known immune pathway ^a	Microarray		qRT-PCR	
			mean ± SEM ^b	p-value	mean ± SEM ^b	p-value
<i>Y19D10A.7</i> <i>F56A4.9^c</i>	Receptor with similarity to human insulin-like growth factor 1 precursor	pnk-1	14.295±0.845	0.0021	13.84±2.208	0.0021
<i>Y19D10A.4</i> <i>C01B4.7^c</i>	Permease of the major facilitator superfamily, similar to human sialin	pnk-1	4.305±0.1677	0.0003	3.346±0.2054	0.0003
<i>Y19D10A.16</i> <i>C01B4.6^c</i>	Similar to human Aldose 1-epimerase	pnk-1	4.272±0.4356	0.0001	5.941±0.3604	0.0001
<i>nspb-1-5</i>	Nematode Specific Peptide family, group B		4.246±1.256	ND	ND	ND
<i>F43C11.3</i>	None		3.6555±0.4285	ND	ND	ND
<i>nlp-25</i>	Neuropeptide-like protein		3.5235±0.6755	ND	ND	ND
<i>C42D4.3</i>	Fibronectin		3.4845±0.1205	ND	ND	ND
<i>Y19D10A.5</i> <i>C01B4.8^c</i>	Permease of the major facilitator superfamily, similar to human sialin		3.4±0.106	0.0142	2.247±0.3004	0.0142
<i>Y19D10A.11</i> <i>F56A4.12^c</i>	Permease of the major facilitator superfamily, similar to human sialin		3.171±0.263	0.0016	2.826±0.2391	0.0016
<i>nspa-9</i>	Nematode Specific Peptide family, group A		2.9805±0.5015	ND	ND	ND
<i>grt-21</i>	Grt domain, intercellular signalling		2.9605±0.0925	ND	ND	ND
<i>col-97</i>	Cuticle collagen		2.9565±0.4775	ND	ND	ND
<i>col-39</i>	Cuticle collagen		2.9505±0.5555	ND	ND	ND
<i>ZK180.5</i>	Similar to human Diacylglycerol kinase kappa		2.883±0.17	ND	ND	ND
<i>col-62</i>	Cuticle collagen		2.5785±0.2495	ND	ND	ND
<i>clcc-72</i>	C-type lectin		2.51±0.439	ND	ND	ND

^a Genes previously linked to known innate immune pathways (8–11)^b Expression level relative to wild-type^c Five gene cluster duplicated on chromosome V

Table 4

Over-represented gene sets among NPR-1-regulated genes

Gene Set	Genes in Set	Genes in Common	Representation Factor ^a	p-value
<i>Pseudomonas aeruginosa</i> -induced genes (7)	197	12	36.1	3.21×10^{-16}
Intestinally-expressed genes (6)	1947	12	3.6	5.46×10^{-05}
PMK-1-regulated genes (8)	110	8	43.1	1.09×10^{-11}

^aThe representation factor is the number of overlapping genes divided by the expected number of overlapping genes drawn from the group of NPR-1-regulated genes and the group corresponding to a given gene set. For details, see <http://elegans.uky.edu/MA/progs/representation.stats.html>.